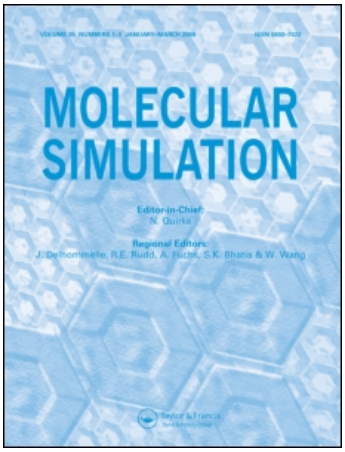

Molecular Simulation
Publication details, including instructions for authors and subscription information:
http://www.informaworld.com/smpp/title~content=t713644482

Barrier properties of small gas molecules in amorphous *cis*-1,4-polybutadiene estimated by simulation

P. Gestoso[a]; M. Meunier[a]
[a] Accelrys Ltd, Cambridge, UK

To cite this Article Gestoso, P. and Meunier, M.(2008) 'Barrier properties of small gas molecules in amorphous *cis*-1,4-polybutadiene estimated by simulation', Molecular Simulation, 34: 10, 1135 — 1141
To link to this Article: DOI: 10.1080/08927020802183559
URL: http://dx.doi.org/10.1080/08927020802183559

Molecular Simulation
Vol. 34, Nos. 10–15, September–December 2008, 1135–1141

Taylor & Francis
Taylor & Francis Group

Barrier properties of small gas molecules in amorphous *cis*-1,4-polybutadiene estimated by simulation

P. Gestoso* and M. Meunier

Accelrys Ltd, Cambridge, UK

(*Received 1 April 2008; final version received 5 May 2008*)

The solubility and diffusivity of small gas molecules in amorphous *cis*-1,4-polybutadiene were estimated in the temperature range 250–400 K, using both molecular dynamics simulations and the transition state theory implementation of the Widom insertion method. A comparison of the methods is given and the results obtained are compared with available experimental data. The accuracy in predicting diffusion and solubility coefficients of a range of small gas molecules in an amorphous polymer of both methods is good when compared to experimental values. The effects of the temperature and the models size are also examined. Selectivity to oxygen and nitrogen are estimated for the various models studied as well. This work shows the potential of computational methods for the prediction of physical properties of industrial importance like selectivity.

Keywords: solubility; diffusion; TST; selectivity; simulation; polybutadiene

1. Introduction

Many industrial applications take advantage of the diverse barrier properties of polymers. Amongst them, gas separation for high purity gases production, food packaging and the beverage industry are most common [1]. More advanced applications are concerned with the development of new polymer membranes for higher selectivity ratio.

Modelling of gas sorption in polymers is a very difficult and presents a permanent challenge to theoreticians and experimenters [2]. The gas permeation process is defined as a 'solution diffusion' process, where at first the gas permeant is dissolved on the surface and then the gas molecules slowly diffuse through the polymer membrane [3]. Predicting the permeability directly from simulation is known to be quite difficult. The advantage of such permeation model is that it allows considering each process (solubility and diffusion) separately and then combining the results to calculate the permeability

$$P = D \times S, \tag{1}$$

where D is the diffusion coefficient and S is the solubility of penetrants [4].

At sufficiently low pressure the solubility is obtained from:

$$C = S \times p, \tag{2}$$

where C is the solubility, p is the pressure and S is the solubility coefficient.

The prediction of physical and chemical properties by computational methods is becoming more and more common in the research area and fortunately computational power is available at a low cost. Various computational methods exist to model amorphous materials (e.g. polymers) that are readily available to the modeller: molecular dynamics (MD), Monte Carlo, transition state theory (TST), mesoscale simulations to name but a few. For a complete review of methods see [5,6]. Recently, MD simulations of up to 3 ns were performed to estimate the diffusivity of small gas molecules in amorphous *cis*-1,4-polybutadiene (*cis*-PBD; [7]).

Polymers are undoubtedly widely used for 'permeation materials' (e.g. in packaging, membrane for gas separation, etc.), due to their chemical resistance. Currently, efforts in research and development concentrate on understanding the phenomena involved during gas transport through membranes, as well as to synthesise novel polymers with better separation properties. The permeability of a specific gas molecule (e.g. O_2) in different polymers varies only slightly. It has been shown that simple relationship can be found between the ratios of the permeability constants for a series of gases through different polymers [8,9]. In fact, it has been shown too that similar relationship can be found for the diffusion and the solubility.

Main factors affecting small penetrants permeability in polymeric material are: the free volume and its distribution [10,11], the density [12], the temperature and pressure, the crystallinity [13], the polymer chain length [12], mobility [14] and packing [10], the solute size [15] and affinity for the material. In addition, computational parameters used

*Corresponding author. Email: patriciag@accelrys.com

ISSN 0892-7022 print/ISSN 1029-0435 online

DOI: 10.1080/08927020802183559
http://www.informaworld.com

in the simulations such as the type of force field employed and the size of the model also affect the permeability value computed [7]. Increase of temperature, generally leads to a decrease of the solubility and conversely for the diffusion. For all three physical quantities P, S and D, the temperature dependence can be described by a Van't Hoff–Arrhenius equation [16]. In particular for the solubility:

$$S(T) = S_0 \exp\left(\frac{-\Delta H_S}{RT}\right), \tag{3}$$

where ΔH_S is the molar heat of sorption.

In this context, this work is oriented towards the assessment of atomistic simulation techniques for the calculation of the barrier properties of *cis*-PBD melts. First, two different methods, MD and TST will be compared in terms of solubility and diffusion coefficients, as well as their capabilities to reproduce their dependence with temperature. Additionally, the effect of chain length on the predictions will be also evaluated. Finally, the ability of both simulation methods to predict selectivity will be compared.

2. Methodology

Computational details of the simulation runs are given in this section, as well as a description of the atomistic models used.

2.1 Models

2.1.1 Short chain models

Polymer models were created using the Amorphous Cell module of the Materials Studio® suite of software [Accelrys Inc., San Diego (2007)] based on the 'self-avoiding' random-walk method of Theodorou and Suter [17] and on the Meirovitch scanning method [18]. Amorphous *cis*-PBD 3D models consisted of 10 chains of 30-monomers oligomers and were equilibrated using a temperature cycle protocol under periodic boundary conditions (Figure 1; [19]). For a full description of the methodology employed to build the equilibrated polymer models at the various temperature of study please see [7].

Polymer models validation was ensured by checking the convergence of the total energy at the end of the MD runs, as well as a density value and cohesive energy density close to that of experiment [7]. Moreover, plotting the total, intra and inter carbon–carbon pair correlation functions (Figure 2) shows that the intra-molecular pair correlation function $g^{CC}_{intra}(r)$ has a limit value of zero and the inter molecular pair correlation function $g^{CC}_{inter}(r)$ has a limit value of one at long range, thus demonstrating well equilibrated configurations.

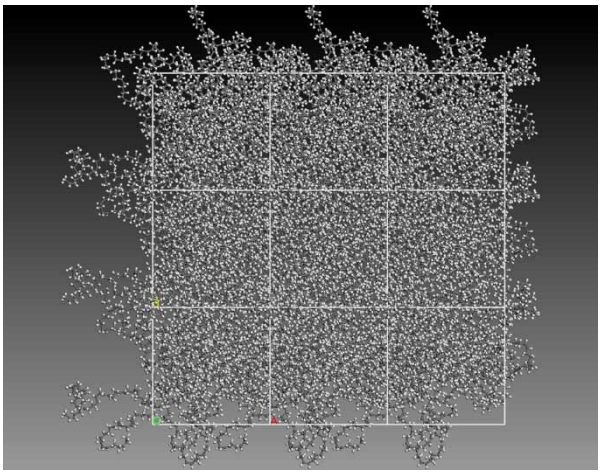

Figure 1. 3D model of amorphous *cis*-PBD at 300 K with periodic boundary conditions.

2.1.2 Long chain models

Polymer models consisting of one single chain of 300 monomers were created using a Monte Carlo based method similar to the short chain models described above. This was done in order to study the effect on diffusion and solubility of the presence in these short chain models of too many chain ends (as compared to the real material), and therefore of added free volume. It has been suggested that this is one of the main factors of discrepancy between simulated and experimental values [7]. The models were validated using similar procedure that described in Section 2.1.1.

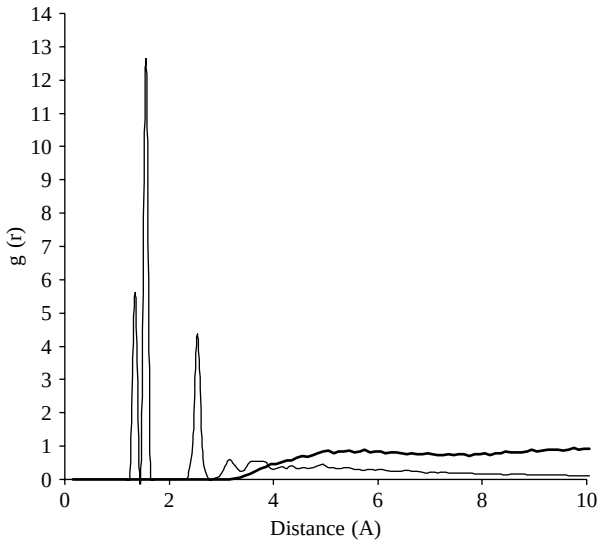

Figure 2. Carbon–carbon pair correlation function (thick line, inter-molecular radial distribution function (RDF); thin line, intra-molecular RDF).

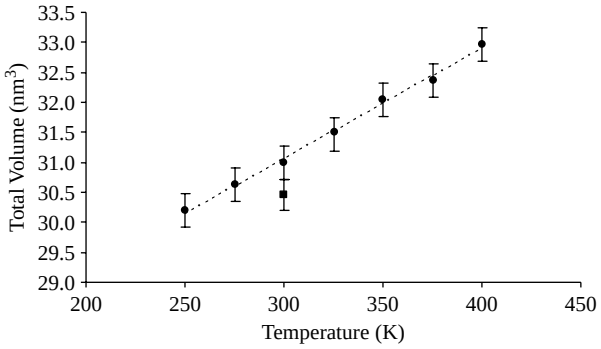

Figure 3. Circles, short chain models polymer total cell volume (average of five frames); square, long chain models (average over five frames).

2.1.3 Sorbates

The geometry of the sorbate molecules were optimised using the DFT code DMol^3 (Accelrys Inc. [20,21]) using default settings. Sorbates were inserted at the same time that the polymer chain using the amorphous cell module (Accelrys Inc.).

2.2 Computational methods

2.2.1 Transition state theory

The TST method was introduced by Arrizi, Gusev and Suter for polymers [22–25]. The method, as implemented in the *InsightII gsnet* and *gdiff* subroutines [26] is initiated as a 3D fine resolution grid laid on the relaxed polymer configuration. Then, a spherical probe of radius equal to that of the gas penetrant is inserted in all grid points and the resulting non-bonded energy, $E_{ins}(x,y,z)$, is calculated between the test probe and all atoms of the polymer matrix. Following the Widom method [27,28] the excess chemical potential, μ_{ex}, is calculated using:

$$\mu_{ex} = RT \ln\left\langle \exp\left(-\frac{E_{ins}}{k_B T}\right)\right\rangle, \tag{4}$$

where R is the universal gas constant, T is the temperature, k_B the Boltzmann constant and the brackets, $\langle\ \rangle$, denote averages over all grid points and probe insertions. Finally, the solubility coefficient is calculated from the excess chemical potential, μ_{ex}, through:

$$S = \exp\left(-\frac{\mu_{ex}}{RT}\right), \tag{5}$$

The identified sorption sites are separated by high-energy barrier surfaces; therefore, penetrant diffusion can be seen as a series of infrequent transitions between adjacent microstates. In TST, in order to calculate the diffusion coefficient the sorbates are displaced in the coarse-grained lattice over a large number of time steps and a large population of ghost walkers through a kinetic MC (kMC) scheme [29,30]. The diffusion coefficient is then calculated from the value of the mean square displacement (MSD) from the trajectories of all penetrant walkers:

$$D = \lim_{t\to\infty}\left\{\frac{\langle[\mathbf{r}_p(t) - \mathbf{r}_p(0)]^2\rangle}{6t}\right\}, \tag{6}$$

where the brackets, $\langle\ \rangle$, indicate average over all trajectories and all time origins. Finally, the permeability is calculated through Equation (1).

The thermal fluctuations of the polymer matrix are taking into account through the smearing factor 'Δ^2', which is related to the MSD of the matrix segments from their equilibrium positions.

The TST method has the advantage of extending the time-scale of the observation when compared to classical dynamics; however, it involves a number of assumptions. First, the polymer matrix response to the guest molecule should be elastic. This is due to the rather simplistic form of calculating the smearing factor, which limits the application of the method to the behaviour of small molecules, which presence does not affect the polymer environment. Second, the shape of the penetrant is supposed to be isotropic. As the penetrant size increases and its shape becomes anisotropic, conventional TST fails to capture the corresponding transport behaviour.

In this work, the grid size used was set to 0.3 Å, in agreement with typical values found in the literature for TST calculations [3,31–34]. The smearing factor, Δ^2, was calculated for each penetrant through a self-consistent scheme involving information about the MSD of all the polymer atoms from their respective equilibrium positions. The MSD was calculated from a 50 ps NVT

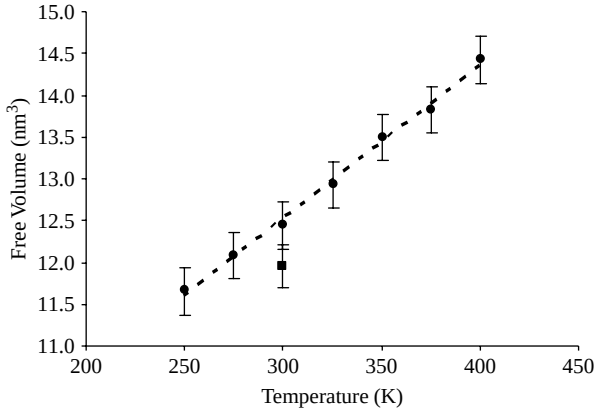

Figure 4. Circles, short chain models polymer free volume (average of five frames); square, long chain models (average over five frames).

MD simulation. The self-consistent scheme converged when the relative difference between two successive Δ^2 values was within 2.5%. The total duration of the kMC procedure was 10^{-4} s and the MSD was averaged over the trajectories of 1000 penetrant walkers.

All penetrant molecules were represented as single, spherical, united-atom sites, whose short-range interactions with the polymer atoms are described through a 9–6 Lennard-Jones potential, the values of collision diameters, σ and the well depths, ε, already reported in the literature for the COMPASS forcefield (Accelrys Inc.) [35]. The non-bonded interactions were truncated at 9.5 Å. All polymer atoms were represented explicitly and the potential function and atomic parameters can be found elsewhere [35]. The reported values correspond to the sampling over five structures and the error bars to standard deviations of the distributions of the calculated values.

2.2.2 *Molecular dynamics*

MD simulations were employed to estimate the diffusion coefficients of the sorbates in both short and long chain models. Four geometry-optimised sorbates were randomly inserted in the model cells and long NVT simulations were performed. The complete methodology has been described elsewhere and is not detailed here [7].

3. Results and discussion

In this part, we report the results of the computation of the solubility values using both Metropolis Monte-Carlo and TST methods. Comparison between the two methods is given, as well as comparison with experimental data when available.

3.1 *General*

We report first the variation of the total and free volume of the models. For the short chain models, the total and free volume are varying linearly with the temperature in the temperature range 250–400 K, as shown on Figures 3 and 4. The free volume represents 38.6% of the total volume at 250 K, 40.2% at 300 K and 43.7% at 400 K. For the long chain models the total free volume represents 39.2% at 300 K, thus slightly less than the short chain models as expected due to a reduction in the number of chain ends at equal density.

3.2 *Solubility coefficients*

The comparison between solubility coefficient results obtained from TST calculations at $T = 300$ K for short and long chain models and experimental results are shown in Table 1. As can be seen, the simulation results follow the experimental tendency, i.e. the solubility parameter increases with the size of the molecule. This behaviour has been well documented in the literature. Additionally, it can be seen that there is a very good quantitative agreement between experiments and TST, especially for long chains, with the exception of CO_2. The failure to capture the CO_2 transport behaviour is inherent to the restrictions of the current implementation of TST where all molecules are considered spherical. As CO_2 has an anisotropic shape, conventional TST fails to capture the corresponding transport behaviour [36].

Table 1. Solubility coefficients ($\times 10^{-6}\,Pa^{-1}$) for various sorbates at $T = 300$ K.

Penetrant	EXP 1 [13]	EXP 2 [37]	TST short-chain	TST long chain
N_2	0.45	0.45	0.74	0.45
Ar	0.76	–	1.13	0.63
O_2	0.96	0.94	1.58	1.18
CH_4	–	–	2.69	1.33
CO_2	9.87	9.7	8.39	3.95
RMSD	–	–	0.418	1.481
RMSD (no CO_2)			0.259	0.085

Comparison of simulation methods and experimental data.

Figure 5 shows the dependence of the solubility coefficient on temperature in the range $250\,K \leq T \leq 400\,K$. As expected, solubility decreases with temperature, i.e. as the temperature increases, the gas molecules experiment more difficulty to condense. This behaviour is in agreement to the experiments (CO_2 in PET [38]) and simulations (CO_2 and He in PE4 [39], CO_2 and CH_4 in polyetherimide [40], CH_4 and CO_2 in HDPE [41], *n*-alkanes in poly(dimethylsilamethylene) [42] and O_2, N_2 and CH_4 in PE for long and short chains [36]).

From Figure 5, it is also possible to calculate the heat of solution. The values obtained were 27.69 kJ/mol for

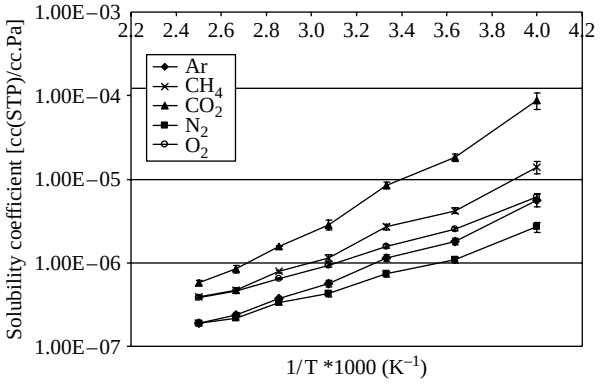

Figure 5. Logarithm of solubility coefficient (in $cm^3(STP)/cm^3\,Pa$) as a function of reciprocal temperature for *cis*-PBD short chain models. (diamond, Ar; cross, CH_4; triangle, CO_2; squares, N_2; circles, O_2).

CO_2, 19.83 kJ/mol for CH_4, 18.53 kJ/mol for Ar, 15.32 kJ/mol for O_2 and 14.54 kJ/mol for N_2. For all penetrants, it was found that the dependence with temperature followed an Arrhenius behaviour (Equation (3)). The fact that the heat of solution values are in general more positive as the solubility of the permeant increases is in contradiction with experimental evidence [37,43], pointing out the limitations of TST to capture the dependence of solubility with temperature.

3.3 Diffusion coefficients

Table 2 presents the comparison between the diffusion coefficients from MD calculations, TST and experimental results at 300 K for short and long chain models. As can be seen, the predicted values from simulations and TST are in good agreement with experimental data, with low values of the RMSD. Deviations are of the same order as in experimental reported data. The experimental reported values of the penetrants in [13] come from two different publications [44] and [45], thus making comparison difficult. Though, the ranking of the penetrants between experiments should be similar, errors while combining data might alter this (as it is the case here for O_2). Overall, theoretical values are systematically overestimating the experimental data; behaviour that has been already observed and reported in the literature [7]. Long chain models perform better than short chain ones, as expected from Figure 3 showing the comparison of free volume in the models. This can be explained as experimental values were measured for very long chain samples, which have smaller free volume and higher density when compared to short chains. Free volume and density play a fundamental role in diffusion, as have been demonstrated elsewhere [36]; therefore, it is to expect that the diffusion coefficient values obtained for the long chain models are closer to experimental values than those from short chain models. Therefore, although, the making of such long chain models is computationally more expensive than the short chain ones, it results in an improvement of the predictability of the methods.

Table 2. Diffusion coefficients for various sorbates ($\times 10^{-6}$) at $T = 300$ K.

Penetrants	Exp [13]	MD long chain	TST long chain	MD short chain [7]	TST short chain
N_2	1.1–2.96	6.11	5.69	8.8	6.08
O_2	1.5	5.07	8.37	9.5	11.19
Ar	4.06	5.06	3.51	7.03	3.84
CH_4	2.25, [10]	2.96	3.22	7.5	3.47
CO_2	1.05	4.06	1.55	5.3	1.58
RMSD		2.58	3.35	5.52	4.59

Comparison of simulation methods and experimental data.

The dependence of diffusion coefficients with the inverse of temperature is plotted in Figure 6 using TST. As can be seen, the diffusivity increases with the temperature, behaviour in perfect agreement with experimental and simulation results in the literature. The diffusion activation energies were calculated as

$$D = D_0 \exp\left(\frac{-E_D}{RT}\right) \tag{7}$$

The values obtained for E_D are 29.70 kJ/mol for CH_4, 29.21 kJ/mol for Ar, 22.11 kJ/mol for O_2 and 26.18 kJ/mol for N_2, which compare well with experimental activation energies in the range of 20–30 kJ/mol [37,43]. This is an improvement compared with the results obtained using MD techniques [7], in which the values for the same penetrants were lower than 10 kJ/mol. For CO_2 the activation energy decreases with temperature as already reported for methane in polybutadiene [7,10].

3.4 Selectivity

A key property for the design of novel material for gas separation is its selectivity. In this paper, we investigate modelling methods to predict the selectivity of small gas molecules in *cis*-PBD. The selectivity is defined as the ratio of the permeability of two penetrants, e.g.

$$\text{Selectivity}\,(O_2, N_2) = \frac{P_{O_2}}{P_{N_2}} = \frac{D_{O_2} S_{O_2}}{D_{N_2} S_{N_2}} \tag{8}$$

where P_{O_2} is the permeability of oxygen and P_{N_2} is the permeability of nitrogen. For the calculations, the MD selectivities were computed from MD diffusion coefficients and TST solubility coefficients for the respective

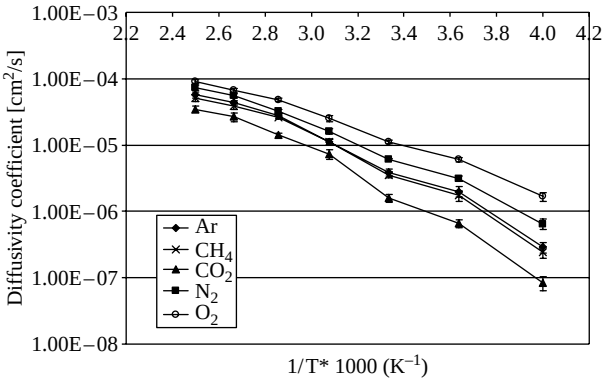

Figure 6. Logarithm of diffusivity coefficient (in cm^2/s) as a function of reciprocal temperature for *cis*-PBD short chain models. (diamond, Ar; cross, CH_4; triangle, CO_2; squares, N_2; circles, O_2).

Table 3. O_2 selectivity at 300 K.

Penetrants	Exp[a] [13]	MD long chain	TST long chain	MD short chain [7]	TST short chain
N_2	0.67	0.46	0.26	0.43	0.25
Ar	2.15	0.53	0.22	0.53	0.25
CO_2	7.27	2.68	0.62	2.96	0.75

[a] Average of both data for N_2.

Table 4. N_2 selectivity at 300 K.

Penetrants	Exp[a] [13]	MD long chain	TST long chain	MD short chain [7]	TST short chain
Ar	3.20	1.16	0.86	1.22	0.96
CO_2	10.81	5.83	2.39	6.83	2.95

[a] Average of both data for N_2.

penetrants, whereas for the TST selectivities both the diffusion and the solubility coefficients where extracted from the TST simulations.

Tables 3 and 4 report the selectivity data from experiment and from simulations. In general, it can be seen that the theoretical models predict correctly the trends for oxygen and nitrogen selectivity. However, in all cases the simulation underestimates the selectivity values when compared to experimental. It is interesting to notice that this underestimation appears to be more noticeable for TST than for MD models.

4. Conclusion

The barrier properties of the *cis*-PBD for different small gas penetrants have been estimated using MD and transition state transition simulations techniques. A molecular model made of one single long chain was created to gain insights on known issues due to incorrect free volume distribution and size in molecular models made of many short chains. There is an overall good agreement between experiments and the results from both methods for solubility and diffusion coefficients; although, as expected, the values corresponding to the long chain models are in better agreement that those from the short chain models. This difference is more noticeable for MD simulations.

The heat of solution and the diffusion activation energy for the different penetrants in *cis*-PBD where derived from the TST plots of solubility and diffusion coefficient vs. temperature, respectively. The heat of solution for the different small molecules did not follow the trends reported in the literature. On the other side, the diffusion activation energies have a very good quantitative and qualitative agreement with experimental values, which was not the case in the MD simulations [7].

Finally, the simulations are able to predict correctly the ranking of the selectivities for oxygen and nitrogen, although, underestimating the values, the TST simulations to a higher degree than the MD simulations.

References

[1] J. Crank and G.S. Park, *Diffusion in Polymers*, Academic Press, London, 1968.

[2] R. Patterson, Y. Yampl'skii, P.G.T. Fogg, A. Bokarev, V. Bondar, O. Ilinich, and S. Shishatskii, *IUPAC-NIST solubility data series 70. Solubility of gases in glassy polymers*, J. Phys. Chem. Ref. Data 28 (1999), pp. 1255–1450.

[3] D. Hofmann, L. Fritz, J. Ulbrich, C. Schepers, and M. Bohning, *Detailed-atomistic molecular modelling of small molecule diffusion and solution processes in polymeric membrane materials*, Macromol. Theory Simul. 9 (2000), pp. 293–327.

[4] Y. Tamai, H. Tanaka and K. Nakanishi, *Molecular Simulation of permeation of small penetrants through membranes*, Macromolecules 27 (1994), pp. 4498–5408.

[5] A.R. Leach, *Molecular Modelling, Principles and Applications*, Pearson Education Limited, London, 1996.

[6] J. Leszczynski, *Computational Chemistry: Reviews of Current Trends*, Jackson State University, MS, USA, 1999.

[7] M. Meunier, *Diffusion coefficients of small gas molecules in amorphous cis-1,4-polybutadiene estimated by molecular dynamics simulations*, J. Chem. Phys. 123 (2005), 134906.

[8] V. Stannett and M. Szwarc, *Rapid determination of oxygen permeability of polymer membranes*, J.Polym. Sci. 16 (1955), pp. 89–91.

[9] H.L. Frisch, *Factorization of the activation energies of permeation and diffusion of gases in polymers*, Polym. Lett. 1 (1963), pp. 581–586.

[10] R.H. Boyd and P.V.K. Pant, *Molecular packing and diffusion in polyisobutylene*, Macromolecules 24 (1991), pp. 6325–6331.

[11] H. Takeushi, R.J. Roe, and J.E. Mark, *Molecular dynamics simulation of diffusion of small molecules in polymers. II. Effect of free volume distribution*, J. Chem. Phys. 93 (1993), pp. 9042–9048.

[12] H. Takeushi, *Molecular dynamics simulations of diffusion of small molecules in polymers: effect of chain length*, J. Chem. Phys. 93 (1990), pp. 4490–4491.

[13] S. Pauly, in *Polymers Handbook*, J. Brandrup and E.H. Immergut, eds., 3rd ed., Wiley, New York, 1989.

[14] H. Takeushi and K. Okasaki, *Molecular dynamics simulation of diffusion of simple gas molecules in a short chain polymer*, J. Chem. Phys. 92 (1990), pp. 5643–5651.

[15] S. Trohalaki, A. Kloczkowski, J.E. Mark, D. Rigby, and R.J. Roe, in *Computer Simulation of Polymers*, R.J. Roe, ed., Prentice-Hall, Englewood Cliffs, NJ, 1991, p. 220.

[16] D.W. Van Krevelen, *Properties of Polymers*, 3rd ed., Elsevier, Amsterdam, 2003.

[17] D.N. Theodorou and U.W. Suter, *Detailed molecular structure of a vinyl polymer glass*, Macromolecules 18 (1985), pp. 1467–1478.

[18] H.J. Meirovitch, *Computer simulation of self-avoiding walks: testing the scanning method*, J. Chem. Phys. 79 (1983), pp. 502–508.

[19] M.P. Allen and D.J. Tidelsey, *Computer Simulation of Liquids*, Oxford University Press, Oxford, 1987.

[20] B. Delley, *An all-electron numerical method for solving the local density functional for polyatomic molecules*, J. Chem. Phys. 92 (1990), pp. 508–517.

[21] B. Delley, *From molecules to solids with the DMol^3 approach*, J. Chem. Phys. 113 (2000), pp. 7756–7764.

[22] S. Arizzi, *Diffusion of small molecules in polymeric glasses: a modelling approach*, Ph.D. thesis, Massachusetts Institute of Technology, Boston, 1990.

[23] A.A. Gusev, S. Arizzi, U.W. Suter, and D.J. Moll, *Dynamics of light gases in rigid matrices of dense polymers*, J. Chem. Phys. 99 (1993), pp. 2221–2227.

[24] A.A. Gusev and U.W. Suter, *Dynamics of small molecules in dense polymers subject to thermal motion*, J. Chem. Phys. 99 (1993), pp. 2228–2234.
[25] A.A. Gusev, F. Müller-Plathe, W.F. van Gunsteren, and U.W. Suter, *Dynamics of small molecules in bulk polymers*, Adv. Polym. Sci. 116 (1994), pp. 207–247.
[26] *Accelrys InsightII*, Accelrys Software Inc., San Diego, 2007.
[27] B. Widom, *Some topics in the theory of fluids*, J. Chem. Phys. 39 (1963), pp. 2808–2812.
[28] B. Widom, *Potential-distribution theory and the statistical mechanics of fluids*, J. Phys. Chem. 86 (1982), pp. 869–872.
[29] R.L. June, A.T. Bell, and D.N. Theodorou, *Transition-state studies of xenon and sulphur hexafluoride diffusion in silica*, J. Phys. Chem. 95 (1991), pp. 8866–8878.
[30] N.C. Karayiannis, V.G. Mavrantzas, and D.N. Theodorou, *Diffusion of small molecules in disordered media: study of the effect of kinetic and spatial heterogeneities*, Chem. Eng. Sci. 56 (2001), pp. 2789–2801.
[31] D. Hofmann, L. Fritz, J. Ulbrich, and D. Paul, *Molecular simulation of small molecule diffusion and solution in dense amorphous polysiloxanes and polyimides*, Comp. Theor. Polym. Sci. 10 (2000), pp. 419–436.
[32] D. Hofmann, L. Fritz, J. Ulbrich, and D. Paul, *Molecular modelling of amorphous membrane polymers*, Polymer 38 (1997), pp. 6145–6155.
[33] E. Kucukpinar and P. Doruker, *Molecular simulations of small gas diffusion and solubility in copolymers of styrene*, Polymer 44 (2003), pp. 3607–3620.
[34] N.C. Karayiannis, V.G. Mavrantzas, and D.N. Theodorou, *Detailed atomistic simulation of the segmental dynamics and barrier properties of amorphous poly(ethylene terephthalate) and poly(-ethylene isophthalate)*, Macromolecules 37 (2004), pp. 2978–2995.
[35] H. Sun, *COMPASS: An* ab initio *force-field optimized for condensed-phase applications-overview with details on alkane and benzene compounds*, J. Phys. Chem. B 102 (1998), pp. 7338–7364.
[36] P. Gestoso and N.Ch. Karayiannis, *Molecular simulation of the effect of temperature and architecture on polyethylene barrier properties*, J. Phys. Chem. B 112 (2008), pp. 5646–5660.
[37] G.J. van Amerongen, *The permeability of different rubbers to gases and its relationship to diffusivity and solubility*, J. Appl. Phys. 17 (1946), pp. 972–985.
[38] Y. Mi, X. Lu, and J. Zhou, *Gas diffusion in glassy polymers by a chain relaxation approach*, Macromolecules 36 (2003), pp. 6898–6902.
[39] N.F.A. van der Vegt, *Temperature dependence of gas transport in polymer melts: molecular dynamics simulations of CO_2 in polyethylene*, Macromolecules 33 (2000), pp. 3153–3160.
[40] S.Y. Lim, T.T. Tsotsis, and M. Sahimi, *Molecular simulation of diffusion and sorption of gases in an amorphous polymer*, J. Chem. Phys. 119 (2003), pp. 496–504.
[41] N. von Solms, J.K. Nielsen, O. Hassager, A. Rubin, A.Y. Dandekar, S.I. Andersen, and E.H. Stenby, *Direct measurement of gas solubilities in polymers with a high-pressure microbalance*, J. Appl. Polym. Sci. 91 (2004), pp. 1476–1488.
[42] V.E. Raptis, I.E. Economou, D.N. Theodorou, J. Petrou and J.H. Petropoulos, *Molecular dynamics simulation of structure and thermodynamic properties of poly(dimethylsilamethylene) and hydrocarbon solubility therein: towards the development of novel membrane materials for hydrocarbon separation*, Macromolecules 37 (2004), pp. 1102–1112.
[43] R. Cowling and G.S. Park, *Permeability, solubility and diffusion of gases in amorphous and crystalline 1,4-polybutadiene membranes*, J. Membrane. Sci. 5 (1979), pp. 199–207.
[44] E.A. Hegazy, T. Seguchi, and S. Machi, *Radiation-induced oxidative degradation of poly(vinyl chloride)*, J. Appl. polym. Sci. 26 (1981), pp. 2947–2957.
[45] E-S.A. Hegazy, T. Seguchi, K. Arakawa, and S. Machi, *Radiation-induced oxidative degradation of isotactic polypropylene*, J. Appl. Polym. Sci. 26 (1981), pp. 1361–1372.